Polish J. Chem., **78**, 1733–1751 (2004) **REVIEW ARTICLE**

Contribution of Electrochemistry to the Knowledge on Structure and Properties of Amalgams*

by C. Gumiński

Laboratory of Chemical Electroanalysis, Department of Chemistry, University of Warsaw, Pasteura 1, 02-093 Warszawa, Poland
E-mail: cegie@chem.uw.edu.pl

(Received February 23rd, 2004; revised manuscript May 25th, 2004)

The most contemporary shapes of the binary phase diagrams of mercury with all elements are displayed in an integral form. Such presentation allows to follow changes of the phase diagram boundaries in the groups and periods of the periodic table of elements. Selection of the critically assessed solubilities of elements is given in a tabular form. Formation of intermetallic compounds, when two metals are introduced into mercury, is briefly characterized. Our knowledge on these fields of interest was considerably extended by the use of various electrochemical techniques. Diffusion coefficients of metals in mercury are mainly determined by electrochemical methods. An analysis of the diffusion data contributes with important informations about structure of simple amalgams; these conclusions are confirmed by other physico-chemical measurements. A liner dependence is observed between logarithms of the standard rate constants of discharging of aquo-ions on mercury electrode and the metal solubilities in mercury.

Key words: mercury binary phase diagrams, solubilities of elements in mercury, reactions and equilibria in complex amalgams, diffusion coefficients of metals in mercury, kinetics of discharge of metal ions on mercury electrode

Introduction

It is impossible to imagine the fast progress in electrochemistry, especially in the middle of XX century, without use of mercury (Hg) electrodes. Simultaneously, a gigantic body of information about Hg binary and ternary alloys (amalgams) was acquired with the application of electrochemical methods. The mutual relations between electrochemistry and amalgams are certainly more frequent on scientific than industrial field. Investigations of many Hg alloys, due to the noble character of Hg and relatively easy studies at room temperature, provided formulation of fundamentals of liquid metal science and metallurgy. Contemporarily, Hg is still the quite important element in various technologies [1], however, due to the well known toxicological aspects, its applications are restrained every year.

Binary Hg phase diagrams

Thermal analysis and X-ray diffraction studies are the most popular ways of investigation leading to construction of phase diagrams, however, in case of Hg as the component, electrochemistry is an equally important tool in such research. Actually,

* Dedicated to Prof. Dr. Z. Galus on the occasion of his 70th birthday.

we know majority of phase relations of the binary Hg systems with metallic and non-metallic elements. This kowledge was critically assessed in recent reviews of the individual phase diagrams and in the monograph on solubility of metals in Hg [2]. The up-to-date outlines of these diagrams are collected in Figs. 1 to 4. They will be further briefly commented taking into account changes of their features in the groups. The experimentally well-documented phase boundaries are plotted with continuous lines. The dashed lines reflect situations where either investigations furnished uncertain informations or boundary lines are predicted according to the thermodynamic rules for construction of the diagrams. Hg melts at 234.3210 K and boils at 629.773 K when pressure is 0.101325 MPa; the horizontal lines in majority of the diagrams reflect these facts when miscibilities of Hg with another elements are very limited.

Since no systematic investigations were performed for the Hg–H system, the corresponding diagram is sketched on basis of fragmentary informations [3]. Both compounds HgH and Hg_2H_2 are stable to practically the same temperature. The solubility of H in liquid Hg (see Table 1) was estimated from precise coulometric experiments. Most probably H exists in liquid Hg in the molecular form.

Table 1. Critically evaluated values of the solubilities of elements in mercury and the equilibrium solid phases at 298 K (the symbols in the parentheses denote solid elements saturated with small amounts of Hg); references are given in the brackets.

Element	Solubility / mol %	Equilibrium phase
H	10^{-7}–10^{-6} [3]	H_2 [3]
Li	1.3 [2]	Hg_3Li [2]
Na	5.38 [5]	Hg_4Na [5]
K	2.53 [2]	$Hg_{11}K$ [2]
Rb	3.2 [2]	$Hg_{11}Rb$ [2]
Cs	4.4 [2]	$Hg_{11}Cs$ [2]
Be	~2×10^{-6} [104]	Hg_2Be or (Be)[11]
Mg	2.7 [2]	Hg_3Mg [12]
Ca	1.0–1.5 [2]	$Hg_{8-11}Ca$ [13]
Sr	2.5 [2]	$Hg_{11}Sr$ [14]
Ba	0.49 [2]	$Hg_{11}Ba$ [15]
La	1.4×10^{-2} [2]	$Hg_{6.5}La$ [17]
Ce	9×10^{-3} [2]	$Hg_{6.5}Ce$ [20]
Pr	1.1×10^{-2} [2]	$Hg_{6.5}Pr$ [21]
Nd	6×10^{-3} [2]	$Hg_{6.5}Nd$ [22]
Sm	2×10^{-2} [2]	$Hg_{6.5}Sm$ [24]
Eu	0.1 [2]	$Hg_{\sim10}Eu$ [25]
Gd	7×10^{-3} [2]	$Hg_{45}Gd_{11}$ [26]
Tb	1.3×10^{-3} [2]	$Hg_{45}Tb_{11}$ [27]
Dy	1.2×10^{-3} [2]	Hg_3Dy [28]
Ho	9×10^{-4} [2]	Hg_3Ho [29]
Er	6×10^{-4} [2]	Hg_3Er [30]
Tm	4×10^{-4} [2]	Hg_3Tm [31]
Yb	0.1 [2]	$Hg_{51}Yb_{14}$ [32]

Table 1 (continuation)

Lu	3×10^{-4} [2]	Hg_3Lu [33]
Th	1.5×10^{-3} [2]	Hg_3Th [35]
U	4.5×10^{-3} [2]	$Hg_{45}U_{11}$ [37]
Pu	1.5×10^{-2} [2]	$Hg_{45}Pu_{11}$ [39]
Ti	2×10^{-5} [2]	Hg_3Ti [42]
Zr	6×10^{-6} [2]	Hg_3Zr [43]
V	$\sim10^{-10}$ [2]	(V) [45]
Nb	10^{-9} [2]	(Nb) [46]
Ta	10^{-8} [2]	(Ta) [47]
Cr	10^{-6} [2]	(Cr) [49]
Mo	$<<10^{-6}$ [2]	(Mo) [50]
W	$<<10^{-6}$ [2]	(W) [51]
Mn	4.5×10^{-3} [2]	Hg_5Mn_2 [52]
Re	$<<10^{-5}$ [2]	(Re) [54]
Fe	10^{-7} [2]	(Fe) [55]
Ru	$\sim10^{-7}$ [2]	(Ru) [56]
Os	$<<10^{-5}$ [2]	(Os) [57]
Co	10^{-7} [2]	(Co) [58]
Rh	1×10^{-4} [2]	Hg_5Rh [60]
Ir	$<<10^{-5}$ [2]	(Ir) [59]
Ni	2×10^{-7} [2]	Hg_4Ni [62]
Pd	3.8×10^{-3} [65]	Hg_4Pd [63]
Pt	5×10^{-4} [65]	Hg_4Pt [66]
Cu	1.00×10^{-2} [2]	Hg_6Cu_7 [67]
Ag	7.6×10^{-2} [2]	$Hg_{15}Ag_{11}$ [68]
Au	0.14 [65]	$HgAu_2$ [69]
Zn	6.32 [2]	$HgZn_{\sim3}$ [70]
Cd	9.53 [2]	$HgCd_{0.3-3}$ [71]
Al	1.6×10^{-2} [2]	(Al) [73]
Ga	3.4 [2]	(Ga) [74]
In	70.0 [2]	$HgIn_{6-11}$ [75]
Tl	42.7 [2]	(βTl) [76]
Si	$<<10^{-5}$ [78]	(Si) [78]
Ge	3×10^{-7} [2]	(Ge) [79]
Sn	1.26 [2]	$HgSn_{6-7}$ [80]
Pb	1.63 [2]	$HgPb_{2-3}$ [81]
N	$<<10^{-3}$ [82]	N_2 [82]
As	2×10^{-9} [2]	(As) [84]
Sb	5×10^{-4} [2]	(Sb) [85]
Bi	1.3 [2]	(Bi) [86]
Se	10^{-6} [89]	HgSe [89]
Te	1×10^{-4} [90]	HgTe [90]
Cl	$\sim10^{-6}$ [93]	Hg_2Cl_2 [93]
Br	$\sim10^{-6}$ [94]	Hg_2Br_2 [94]
I	$\sim10^{-7}$ [95]	Hg_2I_2 [95]
Xe	2×10^{-7} [98]	Xe [98]

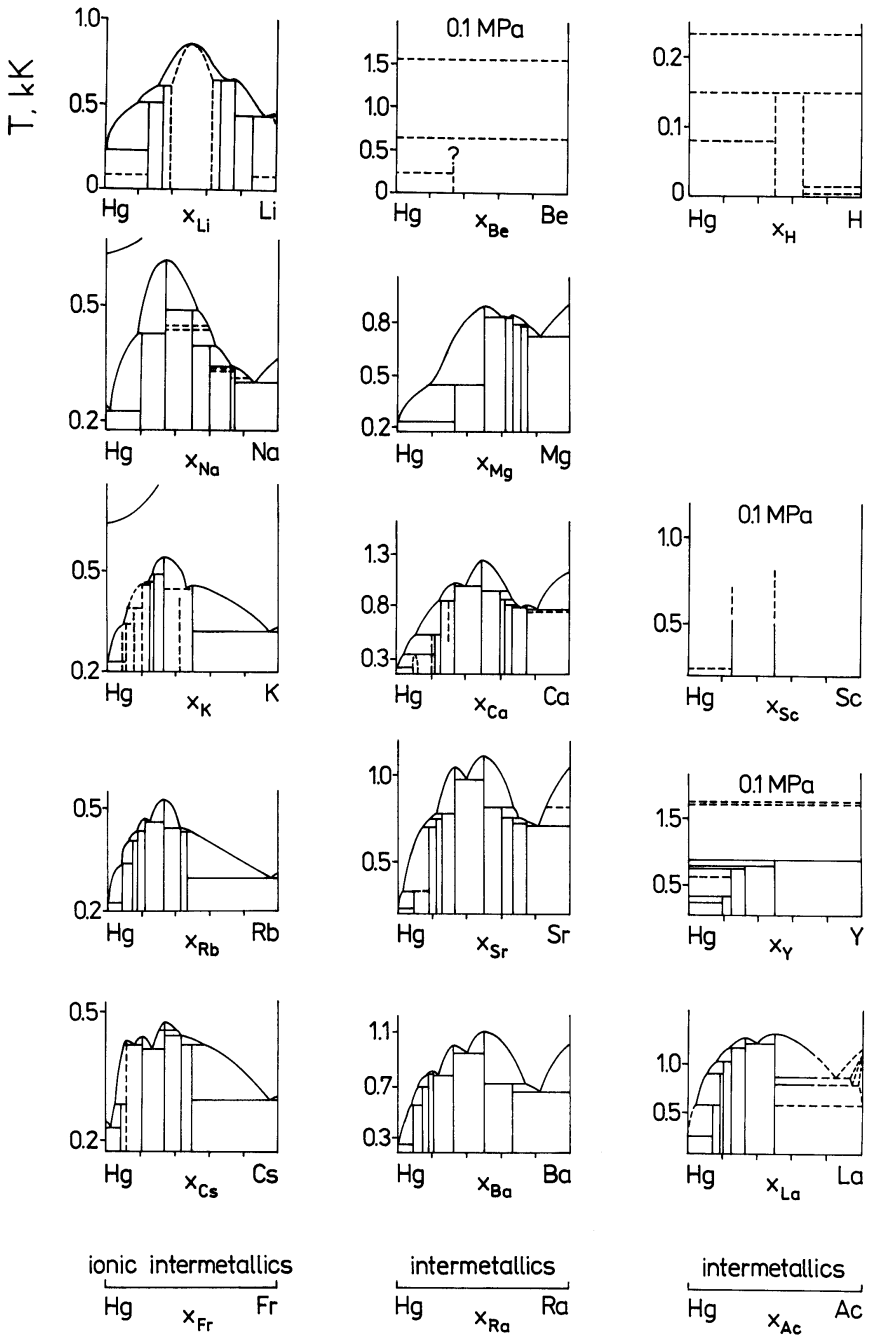

Figure 1. Phase diagrams of binary mercury alloys with s^1, s^2 and d^1 metals. Temperature scales are expressed in kK and compositions are in mol fraction.

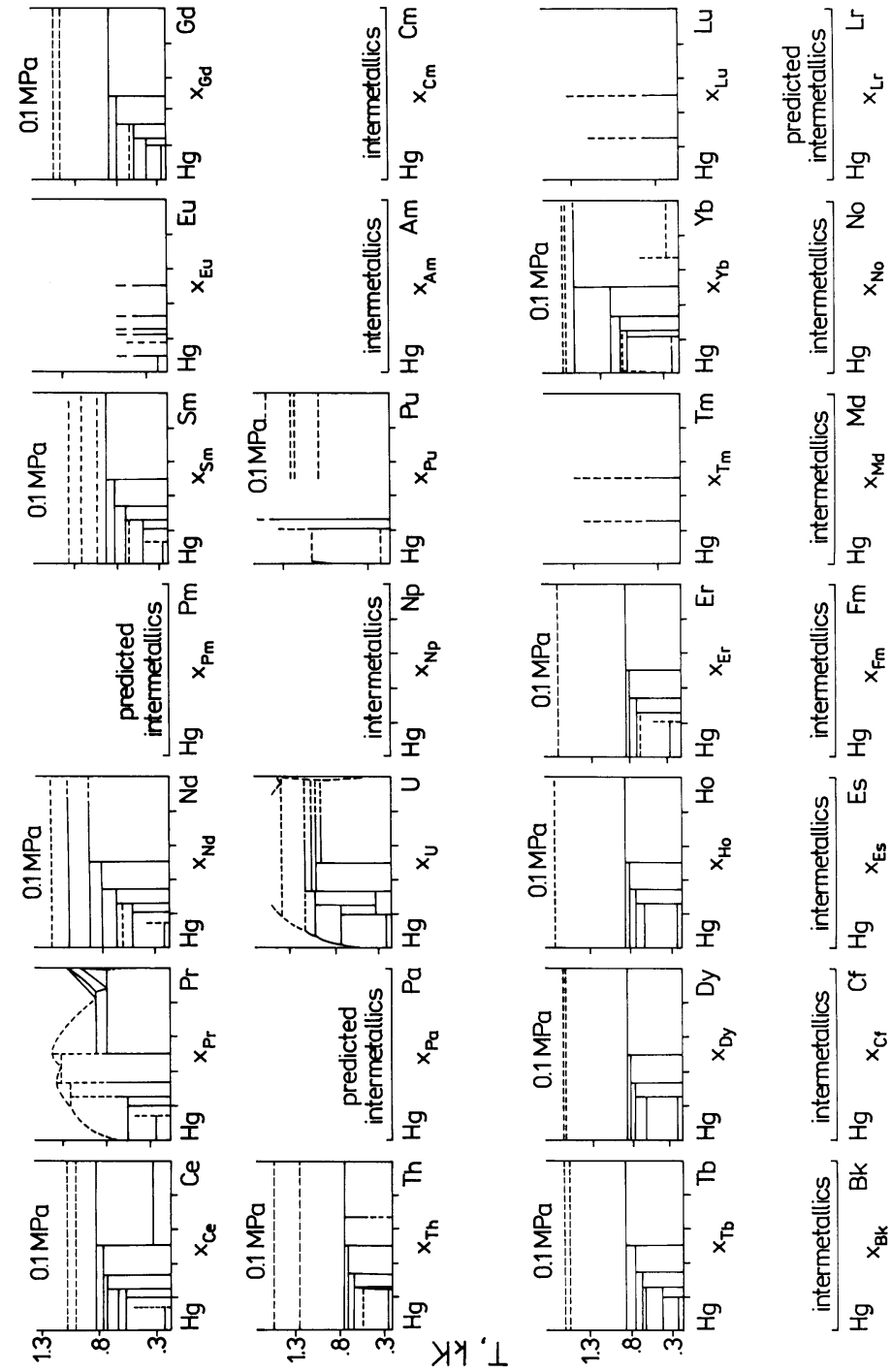

Figure 2. Phase diagrams of binary mercury alloys with f metals.

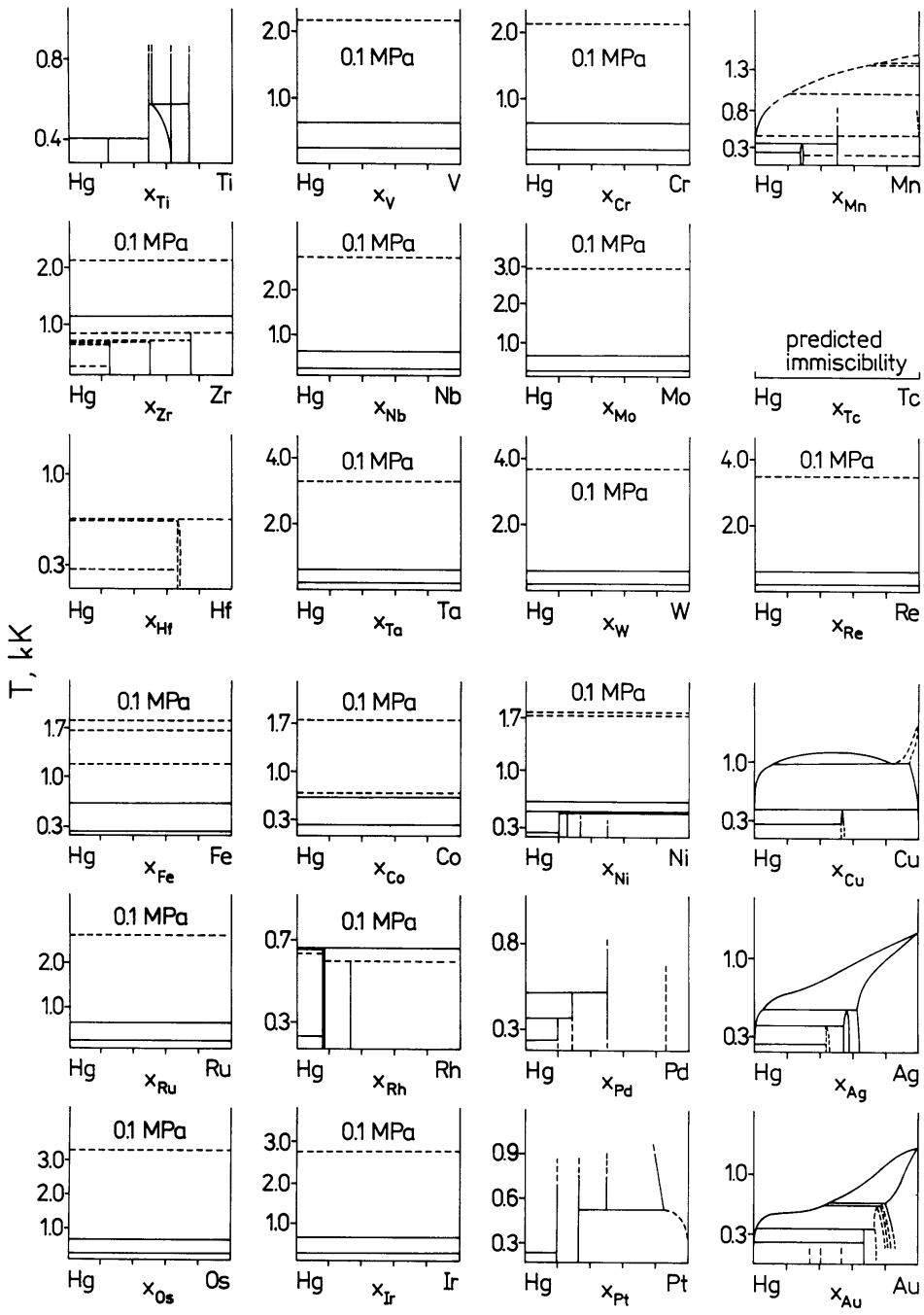

Figure 3. Phase diagrams of binary mercury alloys with d metals.

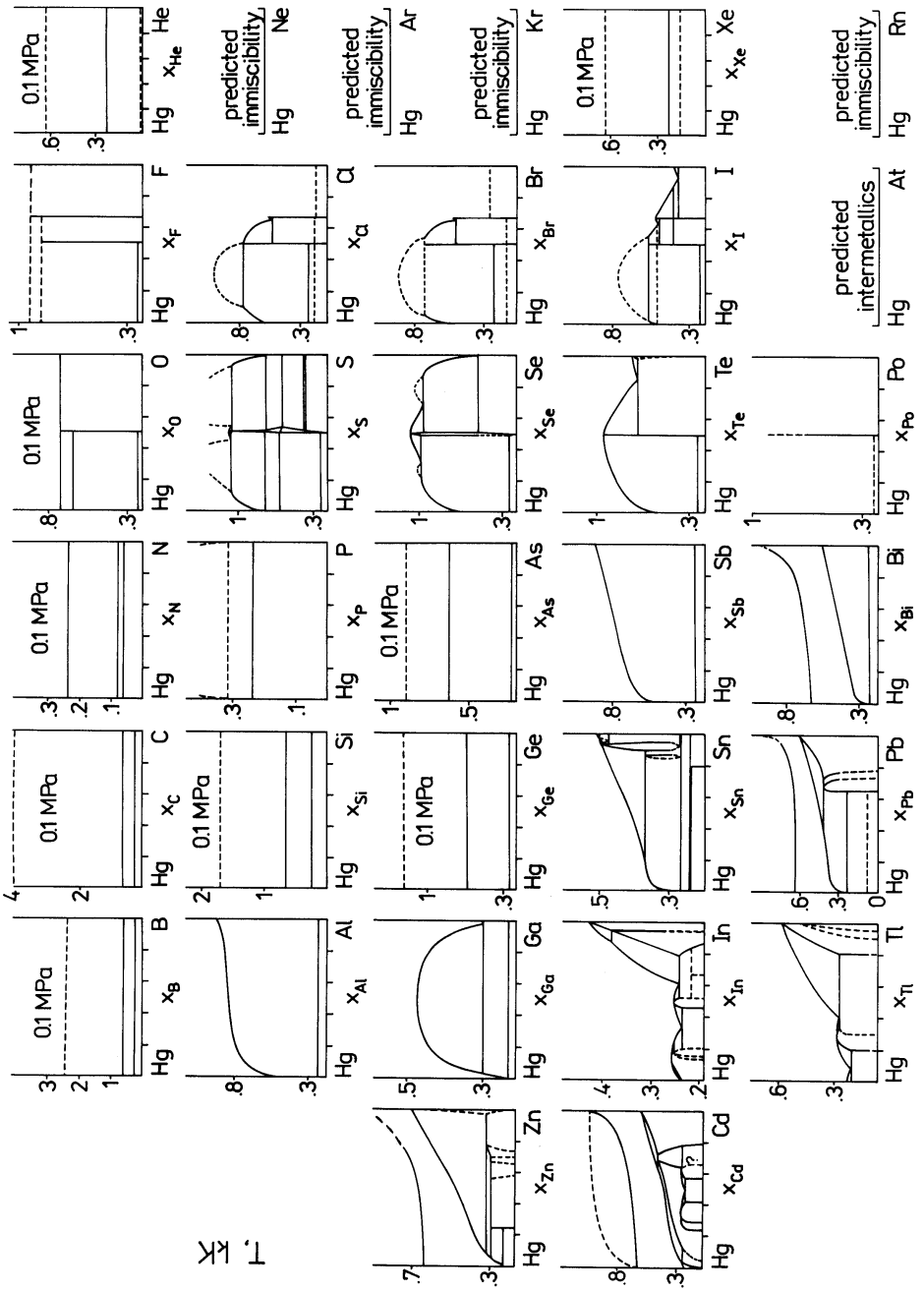

Figure 4. Phase diagrams of binary mercury systems with d^{10} and p elements.

The alkali metals react easily with Hg and sets of intermetallic compounds are formed. Stepping from Li to Cs the bonding between the alkali metal and Hg has more ionic character and, as it was shown in the Knight shift measurements [4], the complete transfer of electron from Fr to Hg occurs in their alloy. The phase diagrams of the alkali metals with Hg are known quite precisely [2,5]; see Fig. 1. One may well observe that an increase of the metal atomic number favors formation of the Hg-rich compounds. Since majority of the experiments related to these phase diagrams was carried out at the beginning of the previous century, some their boundary lines should be verified. Contemporary reinvestigations of the Hg–Na system [5–7] revealed one different stoichiometry and new polymorphic transitions of the compounds which were not reported earlier. Potentiometry and chronoamperometric oxidation were very useful in determination of the liquiduses, compositions of the solid phases and thermodynamic functions of the alkali metals amalgams [2,5,7–10].

The alkaline earth metals react even more pushfully with Hg than the alkali metals do. By similarity to the alkali metals, the formation of the Hg-rich compounds is thermodynamically favorized with an increase of the atomic number of the metal within this group [2,11–15]; see Fig. 1. The most typical stoichiometries observed are: Hg_2M, HgM (the most stable) and HgM_2. Our knowledge on the Hg–Be system, gathered from physico-chemical experiments, is fragmentary and uncertain [11]. A formation of Hg_2Be was suggested on a narrow experimental basis. This suggestion was additionally supported by the fact that the polarographic Be(II) reduction half-wave potential is 0.42 V more positive than the Be(II)/Be standard potential [16]. If the electrode proces is reversible and free from side reactions then $\Delta\hat{G}^{ex}_{Be}$ (the partial excess free energy for diluted amalgam formation) would be ~ –80 kJ/mol Be. Such negative value is only possible when Be affinity to Hg is strong enough to form their intermetallic compound. By similarity, the analogical potential difference in case of Ra amounts 1.32 V [16] and the estimated $\Delta\hat{G}^{ex}_{Ra}$ is then ~ –250 kJ/mol Ra; the half-wave potential of Ra(II) reduction was obtained from radiopolarographic measurements of a very diluted Ra(II) solution. The $\Delta\hat{G}^{ex}_{Ra}$ value is more negative than in the case of Ba what allows to predict a formation of the Hg–Ra compounds (rich in Hg) being more stable than in the Hg–Ba system. Techniques of potentiometry and chronoamperometric oxidation of an amalgam were used to determinations of the solubility of Mg and Ba in Hg [2], respectively. Potentiometry was also used to precise determination of the thermodynamic functions of Mg, Ca, Sr and Ba diluted amalgams [8].

Amalgams of the next group (d^1) from Sc to Ac, with exception of La, were experimentally less investigated; see Fig. 1. The solubility of La in liquid Hg was determined with the use of potentiometry and amperometric oxidation [17]. The stability of the Hg–La compounds is similar to those of Hg with the alkaline earth metals what is reflected by the strongly negative value of $\Delta\hat{G}^{ex}_{La}$ obtained from potentiometric measurements. If one compares the Hg–Sc [18], Hg–Y [19] and Hg–La [17] phase diagrams at pressure of 0.1 MPa one observes quite similar stability of Hg_3M and HgM compounds. Taking this as a rule one may predict an

existence of Hg_3Ac and HgAc compositions, however $\Delta\hat{G}^{ex}_{Ac}$, that is derived from the radiopolarographic half-wave potential and the standard potential of Ac [16], is only one third of the value observed for La. Therefore relatively less stable Hg–Ac compounds are expected.

By similarity to La, all lanthanides (Ln) show distinct affinities to Hg [20–33]. The most typical stoichiometries of the compounds formed are Hg_3Ln and HgLn; see Fig. 2. However, the lighter Ln is the higher is its tendency to formation of the Hg-rich compounds. Certain exclusion from this rule is manifested by Eu and Yb. Both metals display stable valency 2 what makes them similar to the alkaline earth metals. In fact the stoichiometries of the compounds formed in the Hg–Eu and Hg–Yb alloys are typical for the Hg–Ca, Hg–Sr and Hg–Ba systems; see Fig. 1 for the comparison. As it is shown for the La (Fig. 1) [17] and Pr (Fig. 2) [21], an increase of pressure over these alloys (in close capsule experiments) elevates the melting (decomposition) temperatures for up to 400 K. Neither thermal stability of the Hg–Ln compounds nor the $\Delta\hat{G}^{ex}_{Ln}$ values determined from potentiometric data for Ce [20], Pr [21], Nd [22], Sm [24], Eu [25], Gd [26], Ho [29] and Yb[32] show any pronounced tendency with changes of their atomic number [16].

Intermetallics formed in the amalgams of actinides (An) [34–41] seem to be amenable by the similar rules as it was observed for Ln. Unfortunately, we know sufficiently only the Hg–Th, the Hg–U and a part of the Hg–Pu phase diagram. Moreover, Th does not form $Hg_{45}An_{11}$ compound as U and Pu do, and the formula $HgAn_2$ is only observed for Th what may reflect certain individuality of these elements what is also manifested in their chemistry of the valencies higher than 3. It seems that for Cf, Es, Fm, Md and Lr an unified form of the corresponding phase diagram will be observed because they display the typical valency 3. Divalent No should have alloying properties toward Hg analogical to Yb. It is sure that all An elements form stable intermetallics with Hg. Majority of An ions, some of them in the extremal dilution of 10^{-17}–10^{-9} mol/dm^3, was spectacularly investigated with the use of radiopolarography. This technique allowed a determination of their half-wave potentials and, in combination with their standard potentials, an estimation of $\Delta\hat{G}^{ex}_{An}$ values being in the range –130 – –200 kJ/mol An. Although potentiometry was not suitable method for the determination of U solubility in Hg but the electromotive force (emf) measurements in molten salts at higher temperatures led up to precise determination of the thermodynamic properties of the Hg–U system. One should also mention that metallic U, Np and Pu of high purity are effectively produced by the complete reduction from their solutions on Hg cathode and subsequent thermal decomposition of the amalgams obtained [37].

Metals Ti, Zr and Hf show explicit affinity toward Hg [42–44], however they form compounds of different stoichiometries; see Fig. 3. Hf forms only one, but Ti as much as four intermetallics. Ions of these metals are not simply reducible to the zero valency on Hg electrode in aqueous solutions due to the simultaneous hydrogen ion discharge, therefore electrochemical investigations of these amalgams are practically absent in the literature.

For the similar reasons there are no rational experiments performed with amalgams of V, Nb and Ta using electrochemistry. These metals do not form compounds with Hg and are very hardly miscible with it [45–47]; see Fig. 3 and Table 1. The theoretical predictions in [45] suggests that both liquid Hg and V will mix 222 K above the melting point of V (2183 K). Nevertheless, we will not be able to confirm this prediction experimentally because the critical temperature of Hg is at1765 K and over this temperature Hg is in the gaseous or fluidal state and losts its metallic properties [48].

Cr, Mo and W, analogically to the previuos group, form no intermetallics with Hg and are resistant to a dissolution even at elevated temperatures [49–51]; see Fig. 3. The only exception is that Cr(II) is reducible from aqueous solution on Hg electrode, however, potentiometric measurements performed with Cr amalgam failed due to its very low solubility in Hg; see Table 1.

Mn has the half-filled level of $3d^5$ electrons what assimilate its features to the $3d^{10}$ electron configuration of Zn. Therefore Mn is relatively well soluble in Hg and forms two intermetallics with it [52]; see Table 1 and Fig. 3. The low temperature part of the Hg–Mn liquidus was determined with the use of potentiometry as well as amalgam polarography, voltammetric and chronoamperometric oxidation. The emf method was also used for the determination of some thermodynamic parameters of the Hg–Mn system. No experimental material exists for the Hg–Tc system [53] which should be between the Hg–Mn and the Hg–Re. Tc has a different electron configuration ($4d^6 5s^1$) and is in fact more similar to Re than to Mn. Thus any Hg–Tc intermetallics are unlikely to exist and mutual solubilities of the metals should be very small. Due to the strong cohesion forces, Re is very resistant to dissolution in Hg and forms no compounds with it [54].

A very limited miscibility in solid and liquid states and no formation of intermetallics with Hg are reported for the triad Fe, Ru and Os [55–57]; see Fig. 3. Probably, the poor solubilities in Hg decrease with the atomic number of the metals by similarity to the previous groups of the transition metals. Although potentiometry was applied to the determination of Fe solubility in Hg the result obtained was strongly overestimated.

Co and Ir are characterized by the analogic electron structures $3d^7 4s^2$ and $5d^7 6s^2$, respectively, whereas Rh has the $4d^8 5s^1$ configuration. This may be the cause that the first two metals do not react with Hg and are hardly miscible with it [58,59], whereas Rh is relatively better soluble in Hg and forms intermetallics with it [60]; see Fig. 3 and Table 1. Although emf experiments with heterogeneous Co amalgam pointed on its improbably high solubility, then chronopotentiometric and pulse-polarographic oxidation of this amalgam led to quite reliable results. Interactions of Rh and Ir with Hg were variously investigated in order to search new base metals for microelectrodes covered with Hg. No Hg_5Rh (as one could predict from the Hg–Rh phase diagram) but Hg_2Rh is formed after an electrochemical deposition of Hg on Rh [61]. In similar conditions Ir simulates formation of an intermetallic compound with Hg because no complete stripping of Hg is achieved during the oxidation step. It seems

most likely that a formation of Hg–Ir–O mixed oxide or a very strong adsoption keeps a part of Hg on the Ir surface [59].

The alloys of Hg with Ni and Pd (see Fig. 3) were very intensively investigated with electrochemical methods. The stoichiometry of intermetallics formed, HgM and Hg_4M, are observed for both metals and for Pt. The solubility of Ni in Hg, identification of the equilibrium solid phases in the Hg–Ni system and their thermodynamic characterizations were obtained with the use of potentiometry as well as coulometric, voltammetric, chronoamperometric and chronopotentiometric oxidation of Ni amalgams [62]. Compositions of the equilibrium solid phases and the thermodynamic parameters of formation in the Hg–Pd system were determined from chronopotentiometric and voltammetric oxidation of Pd amalgam [63, 64]. The solubilities of Pd and Pt were successfully measured tracing the precipitation of PdZn or $PtZn_2$ in Hg in slow-scan voltammetric and chronopotentiometric conditions [65]. Many electrochemical experiments performed for the Hg–Ni and Hg–Pt systems showed that the related phase equilibria are settled very slowly.

Cu, Ag and Au interact with Hg faster. Therefore the corresponding phase equilibria are better known; see Fig. 3. Cu forms one, Ag – two and Au – more than three intermetallics with Hg but the stoichiometries are different. The Cu solubility in Hg, the stoichiometry of Hg_6Cu_7 and several thermodynamic properties of the Hg–Cu system were determined with the use of potentiometry, amalgam polarography, coulometry, voltammetry and thin film amperometry [67]. The voltammetric oxidation of saturated Ag amalgam in acetonitrile did not lead to the correct solubility value but the potentiometric measurement of a cell with Ag(I) in acetonitrile solution was fruitful [68]. By analogy to Pd and Pt, the Au concentration in its saturated amalgam was determined by the slow-scan voltammetry which traced the precipitation reaction of AuZn in Hg [65]; other features of the Hg–Au phase diagram [69] were obtained by non-electrochemical methods.

Intermediate phases with extended homogeneity ranges are formed in the Hg–Zn [70] and Hg–Cd [71] systems, both metals are relatively well soluble in Hg; see Fig. 4 and Table 1. Potentiometry and chronoamperometric oxidation of Zn amalgam were used for the determinations of Zn solubility in Hg, the solid solubility of Hg in Zn and the thermodynamic properties of the Hg–Zn system. The same techniques were used in the investigation of the Hg–Cd system.

Shapes of phase digrams for the alloys of p^1 elements with Hg change distinctly stepping from B to Tl. B, by an analogy to the high melting transition metals, seems to be very resistive to a dissolution in Hg and interaction with it [72]. Liquid Al mixes with Hg in every proportion [73], however, liquid Ga shows the limiting miscibility with Hg [74]; both metals do not form intermetallics. In oposite, In and Tl are the most soluble metals in Hg at room temperature (see Table 1) and their intermediate phases with Hg are relatively stable [75,76]. Electrochemistry of Al is not simple, however, the use of potentiometry in non-aqueous solvents and amperometric oxidation of Al from a thin Hg film electrode on Al base, allowed to determine the Al solubility in Hg [2]. Electrochemical techniques were also used to estimate the solid solubility of Hg

in Al [73]. It was shown that the Ga solubility may be determined by potentiometry as well as by chronoamperometric and voltammetric oxidation of the saturated amalgam. Potentiometry was applied many times to determine the thermodynamic properties of Ga, In and Tl amalgams [74–76].

Although Hg may be intercalated into graphite in a chemical reaction, graphite itself seems to be the most resistant element for a dissolution in Hg [77]. Stepping down to Si [78] and Ge [79], their solubilities in Hg increase but they are still quite limited; see Table 1. Chronoamperometric oxidation and amalgam polarography of Ge were used for the determination of its solubility. Sn [80] and Pb [81] form intermediate phases with Hg and their solubilities are relatively high. The mutual solubilities and thermodynamic properties of the Hg–Sn and Hg–Pb alloys were investigated by emf and chronocoulometric oxidation.

Although the metastable Hg_3X_2 compounds for N, P, As and Sb were prepared by chemical methods, they are not formed in a direct contact of these elements with Hg [82–85]. Therefore the corresponding phase diagrams as well as of the Hg–Bi system [86] have simple forms. N and As are quite poorly soluble in Hg but P is partly miscible with Hg. Plenty of electrochemical methods was applied (potentiometry, amalgam polarography, chronoamperometric and voltammetric oxidation of the heterogeneous Sb amalgams) for the determination of the Sb solubility in Hg. Electromotive force method was used for the determination of Bi solubility in Hg and the thermodynamic properties of the Hg–Bi system.

A direct contact of O, S, Se, Te or Po with Hg leads exclusively to the compound formation of stoichiometry 1:1; HgS and HgSe have the bertholide-like character. Unexpectedly, no compounds of Hg(I) and of polysulfides and polyselenides, known in chemistry, are reflected in the equilibrium phase diagrams [87–91]; see Fig. 4. HgO, HgS and HgSe are hardly soluble in Hg what was observed by electrochemists long time ago. The determinations of the Se and Te solubilities in Hg by alternating current polarography and chronoamperometric oxidation yielded some overestimated results pointing on the relatively slow crystallization processes and susceptibility of these solutions to a supersaturation. The free energy of HgTe formation was successfully found from coulometric titration experiments.

All halogens form two types of compounds: Hg_2X_2 and HgX_2. Their stabilities decrease with the increase of the atomic number of halogen [92–95]. It is very likely that also At forms moderately stable compounds with Hg [96]. Repeatedly, electrochemists observed unmeasureably small solubility of Hg halides in liquid Hg. An extrapolation of the solubility data from higher temperatures to room temperature, resulted in the solubility values shown in Table 1. Numerous emf investigations allowed precise measurements of the thermodynamic properties of Hg_2X_2 and HgX_2 compounds.

Although excited Hg and noble gases form unstable HgX molecules in the gas phase, no compounds were identified in the condensed states. The solubility of Xe in Hg at room temperature was determined (see Table 1) and solubilities of other noble gases in Hg seem to be likewise negligible [97,98].

Reactions and equilibria in complex amalgams

Some ternary Hg-rich systems were investigated at the beginning of previous century, however, the construction of electrodes with Hg drop hanging on Au tip or Hg film adhering to Ag plate induced immensity of electrochemical investigations related to possible interactions of metals in Hg medium [99]. Diverse methods, such as: potentiometry, amalgam polarography, cyclic and stripping voltammetry, coulometry, chronoamperometry, chronopotentiometry and chronocoulometry with application of various types of electrodes were used for investigation of the equilibria and kinetics of the reactions occurring between metals introduced into Hg. About 200 systems M_1–M_2–Hg were electrochemically investigated and quantitave data were obtained for about 60 systems. Investigations of these equilibria are hindered by a relatively slow kinetics of these reactions.

Generally, if a stable compound is formed in a binary M_1–M_2 system then probability of a formation of such compound in Hg environment is high [100]. Stabilities of the intermetallics formed in Hg are expressed by the well-known solubility product:

$$K_{so} = [M_1]^x [M_2]^y \quad (1)$$

where x and y are stoichiometric coefficients of the compound formula. One may likewise find in the corresponding literature that such equilibria are expressed by the stability constants. However, it was firmly established that the intermetallic compounds are precipitated from Hg solution when a product of concentrations of both metals overruns the solubility product.

Diffusion coefficients and structure of simple amalgams

Diffusion coefficients in liquid metallic systems may be determined by several physico-chemical methods, however in the case of metals dissolved in Hg the application of electrochemical techniques is dominant. A metal, less noble than Hg, may be oxidized from a stationary Hg drop or pool electrode in chronoamperometric, voltammetric or chronopotentiometric conditions. If an amalgam drops regularly from a capillary it may be then oxidized polarographically [101]. There are also special methods of the investigation. During chronoamperometric reduction of Zn(II) on an Au drop amalgam electrode, at potentials of the base of Zn(II) reduction wave, due to the fast reaction between Au and Zn the current recorded depends on the rate of Au diffusion to the electrode surface and the diffusion coefficient of Au may be found [102]. If a metal plate (Al, Cu, Sn) is covered with a thin Hg film then a stationary oxidation current recorded is dependent (among others) on the diffusion coefficient of this metal in Hg what makes possible to determine it [103].

The selected diffusion coefficients of metals in diluted amalgams were beforehand tabulated in [104]. This list may be now supplemented by the recent data for Li and Ca [105], Sr [106], La [107] and Te [108]. The values for K and Sr at 298 K are obtained from an interpolation of the corresponding results at other temperatures.

The all selected values are presented in Fig. 5 in form of the reciprocal diffusion coefficient *vs*. effective radius of the metal. Such way of analysis is originated from the well-known Sutherland-Einstein equation:

$$D_M = k\,T / 4\,\pi\,\eta_{Hg}\,r_M^d \qquad (2)$$

where D_M is the diffusion coefficient of M, k the Boltzmann constant, T temperature, η_{Hg} the viscosity of Hg and r_M^d the radius of the diffusing particle.

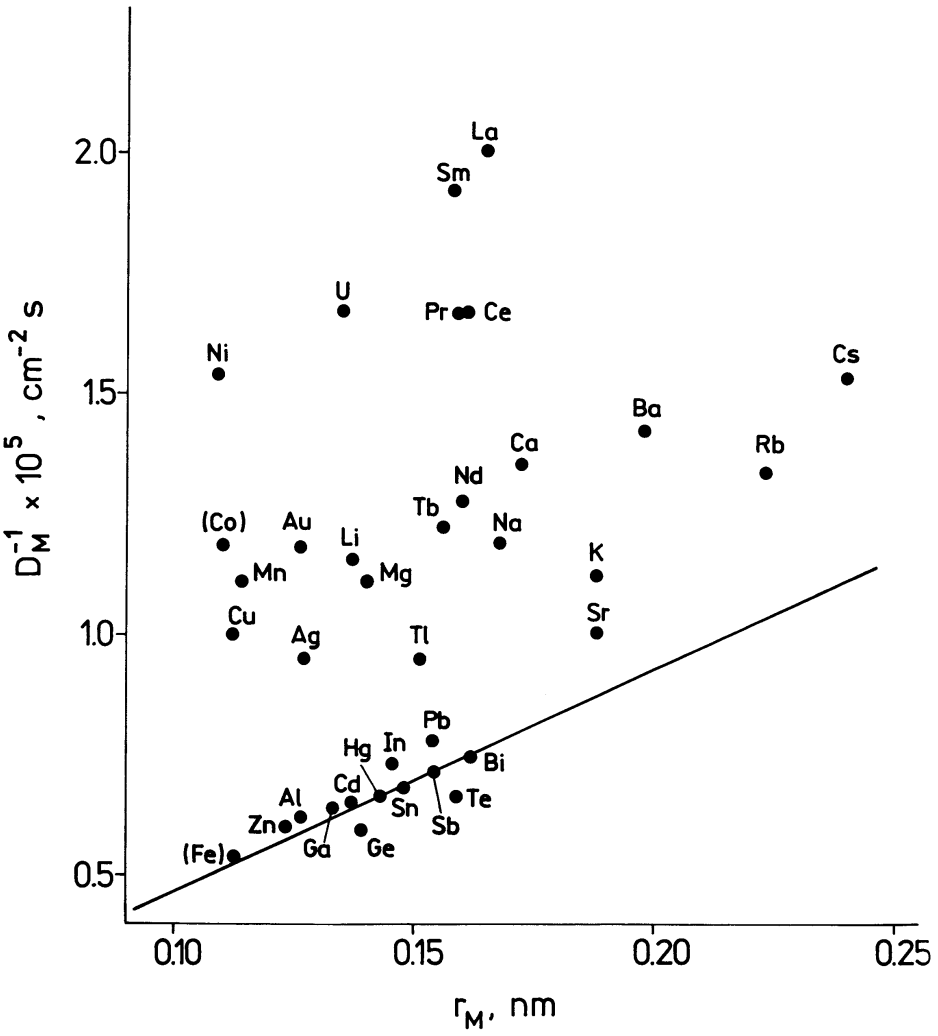

Figure 5. Dependence of the reciprocal diffusion coefficients in mercury at 298 K on the effective metal atom radii.

Correctness of the simple Eq. (2) was verified on the self-diffusion of many liquid metals when the effective r_M was calculated from the molar volume of metal. The metals dissolved in Hg which do not form stable intermetallics with Hg as: Cr, Zn, Al, Ga, Cd, Ge, In, Sn, Pb, Sb and Bi, fulfill quite well Eq. (2). The fulfillment by D_{Fe} as well as the unfulfillment by D_{Co} may be accidental because this author has reservation to the experimental conditions of measurements in [104]. All other metals which form stable intermetallics with Hg are placed over the straightline reflecting Eq. (2) what means that they diffuse as larger entities than atoms. The simplest interpretation of this fact is a postulate that these atoms are surrounded by Hg atoms and as such diffuse in the Hg medium. The radii of the diffusing solvates may be calculated from Eq. (2) and an approximate composition of such diffusing entities estimated. The compositions found this way are frequently similar to the compositions of the solid Hg–M phases which are in equilibrium with the liquid amalgams at 298 K (shown in Table 1) as it was found for example in the case of Hg_3Li. The only exception from this rule is observed for D_{Te}; this coefficient is known accurately but it is placed below the straightline. This suggests that an entity smaller than Te atom (Te^{2+}?) takes part in the Te diffusion process. However, HgTe molecule is quite stable (see Fig. 4) and one may only imagine its possible dissociation to Te^{2-} ion which is still 37 % larger than the Te atom. Thus either we have to do with an unexplained phenomenon or D_{Te}, due to a possible experimental imperfections in [108], is overestimated.

Investigations of liquid amalgams by cyclic voltammetry, chronoamperometry [109], potentiometry [110], X-rays, electrical resistance, thermoelectric power, magnetic susceptibilities and thermodynamic analysis [104] pointed also on the existence of intermetallic molecules in the simple liquid amalgams. This confirms the above presented interpretation of the diffusion coefficients.

Kinetics of dissolution of pure metals and Hg–M alloys in liquid Hg was intensively investigated by electrochemical and physical methods [104]. A part of the processes was diffusion controlled and the rest was slower, however no any rational correlation of the kinetic constants measured with the kind of metal or alloy was established.

Kinetics of discharging metallic cations on Hg electrode

Tamamushi [111] observed that the rate constant of reduction of a metal aquo-ion with an amalgam formation is at the best correlated with the solubility of the metal in Hg but neither with the free energy of ion hydration, the free energy of metal amalgamation nor the rate constant of exchange of water molecule in the first solvation sphere. This unexpected observation was further confirmed with larger number of metals tested in [104]. The most recent correlation between logarithm of the rate constant of the electrode proces and logarithm of the metal solubility in Hg is presented in Fig. 6. The most recent kinetics data for Mg, Ca, Ba, Sm, Eu and Yb are quoted from [112] and for H from [3]. The case of In(III), which is quite slowly reduced, is the most deviating from the straightline dependence. It is possible that if one would consider In(I) reduction instead of In(III), by analogy to Tl(I), then the rate

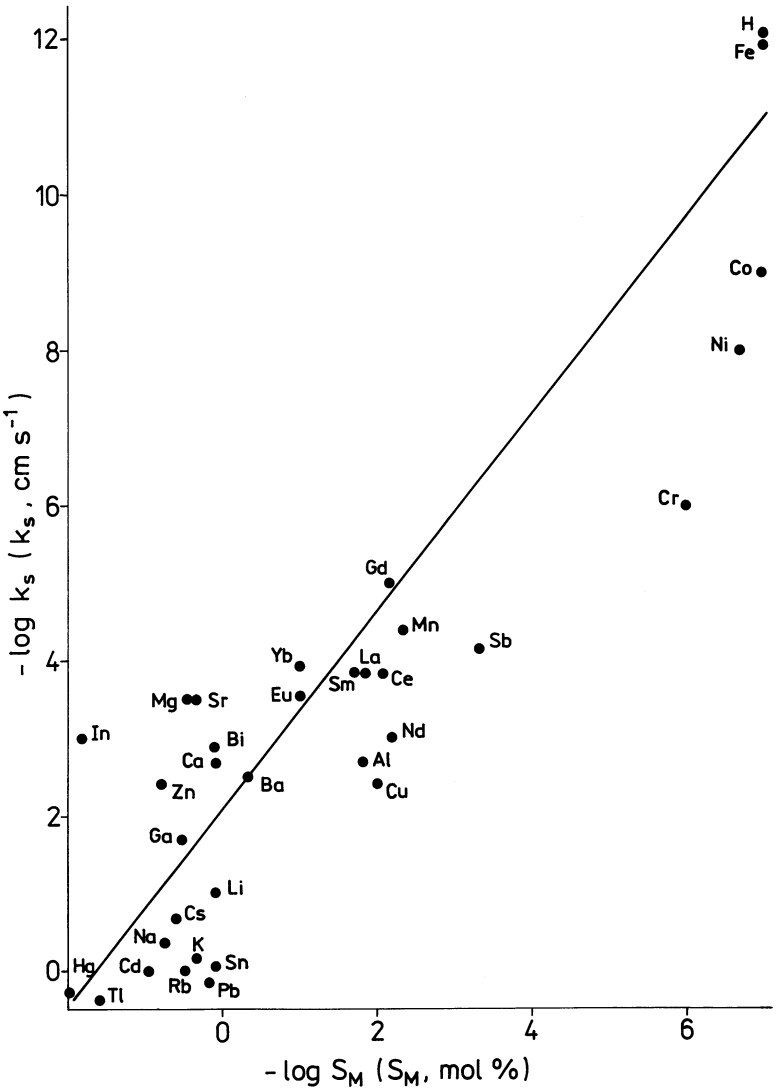

Figure 6. Bi-logarithmic dependence of the rate constant of aquo-ion reduction to the amalgam state on the metal solubility in mercury at 298 K.

constant for In(I) would be much higher and the corresponding point for In placed nearer to the straightline. Based on this empirical dependence, one may predict an approximate value of the rate constat of electroreduction of aquo-ion to the amalgam state if one knows the metal solubility in Hg.

Acknowledgments

The author is greatly indebted to Prof. Zbigniew Galus; without his introduction into the world of amalgams and the innumerable helpful discussions, this as well as the most of the referred papers would not come into being. The program of binary mercury phase diagrams evaluation (ASM/NIST) was initiated by Prof. Thaddeus B. Massalski; his encouragement and valuable advices are kindly acknowledged. Thanks to Prof. Jack F. Smith for numerous discussions and intense help in the lingustic improvement of individual assessments. Sincere gratitude is directed to Dr. Hiroaki Okamoto, Dr. William W. Scott and all ladies in the ASM office for the support and fruitful co-operation. At last but not least, thanks to Prof. Zbigniew Moser and Dr. Leszek A. Zabdyr for the perfect team-work.

REFERENCES

This is the list of general references and in case of need a reader interested in more specific papers should inspect further references inserted therein.

1. Gumiński C., *Amalgams*, in *Intermetallic Compounds*, Vol. 3, J.H. Westbrook and R.L. Fleischer, Eds., Wiley, Chichester, 2002, p. 21.
2. Gumiński C. and Galus Z., *Metals in Mercury*, *IUPAC Solubility Data Series*, Vol. 25, C. Hirayama, Ed., Pergamon, Oxford, 1986.
3. Gumiński C., *J. Phase Equil*., **23**, 448 (2002).
4. Haas H., Stenzel Ch., Mahnke H.E., Spellmeyer B. and Zeitz W.D., *Hyperfine Interactions*, **60**, 675 (1990).
5. Borgstedt H.U. and Gumiński C., *Metals in Liquid Alkali Metals*, *IUPAC Solubility Data Series*, Vol. 64, Oxford University, Oxford, 1996, p. 137.
6. Deiserot H.J., Biehl E. and Rochnia M., *J. Alloys Comp*., **246**, 80 (1997).
7. Sun Ch. and Cao Y., *Acta Metall. Sinica*, Ser. B, **6**, 256 (1993).
8. Mussini T., Longhi P. and Rondinini S., *Ann. Chim*., **73**, 357 (1983).
9. Hultgren R., Desai P.D., Hawkins D.T., Gleiser M. and Kelley K.K., *Selected Values of the Thermodynamic Properties of Binary Alloys*, American Society for Metals, Metals Park, 1973.
10. Kremann R. and Mehr A., *Z. Metallk*., **12**, 444 (1920).
11. Okamoto H. and Tanner L.E., *Phase Diagrams of Binary Beryllium Alloys*, American Society for Metals, Metals Park, 1987, p. 108.
12. Nayeb-Hashemi A.A. and Clark J.B., *Bull. Alloy Phase Diagr.*, **8**, 65 (1987).
13. Gumiński C., *J. Phase Equil*., **14**, 90 (1993).
14. Gumiński C., to be published.
15. Gumiński C., *J. Phase Equil*., **21**, 173 (2000).
16. Nugent L.J., *J. Inorg. Nucl. Chem*., **37**, 1767 (1975); Yamana H. and Moriyama H., *J. Alloys Comp*., **275–277**, 898 (1998).
17. Gumiński C., *J. Phase Equil*., **16**, 186 (1995).
18. Gumiński C., *ibid*., **14**, 391 (1993).
19. Gumiński C., *ibid*., **16**, 277 (1995).
20. Gumiński C., *ibid*., **14**, 382 (1993).
21. Gumiński C., *ibid*., **16**, 454 (1995).
22. Gumiński C., *ibid*., **16**, 448 (1995).
23. Gumiński C., *ibid*., **16**, 526 (1995).
24. Gumiński C., *ibid*., **16**, 86 (1995).
25. Gumiński C., *ibid*., **14**, 97 (1993).
26. Gumiński C., *ibid*., **16**, 181 (1995).
27. Gumiński C., *ibid*., **16**, 193 (1995).
28. Gumiński C., *ibid*., **16**, 73 (1995).
29. Gumiński C., *ibid*., **16**, 77 (1995).
30. Gumiński C., *ibid*., **16**, 177 (1995).
31. Gumiński C., *ibid*., **16**, 459 (1995).
32. Gumiński C., *ibid*., **16**, 348 (1995).

33. Gumiński C., *ibid*., **16**, 276 (1995).
34. Gumiński C., *ibid*., **16**, 332 (1995).
35. Gumiński C., *ibid*., **15**, 204 (1994).
36. Gumiński C., to be published.
37. Gumiński C., *J. Phase Equil*., **24**, 461 (2003).
38. Gumiński C., *ibid*., **20**, 84 (1999).
39. Gumiński C., to be published.
40. Gumiński C., *J. Phase Equil*., **16**, 333 (1995).
41. Gumiński C., *ibid*., **17**, 443 (1996).
42. Murray J.L., *Phase Diagrams of Binary Titanium Alloys*, American Society for Metals, Metals Park, 1987, p. 140.
43. Gumiński C., *J. Phase Equil*., **24**, 469 (2003).
44. Gumiński C., *ibid*., **16**, 334 (1995).
45. Smith J.F., *Bull. Alloy Phase Diagr.*, **6**, 179 (1985).
46. Gumiński C., *J. Phase Equil*., **14**, 388 (1993).
47. Gumiński C., *ibid*., **22**, 684 (2001).
48. Gumiński C., *ibid*., **13**, 657 (1992).
49. Venkatraman M. and Neuman J.P., *Bull. Alloy Phase Diagr.*, **10**, 157 (1989).
50. Gumiński C., *J. Phase Equil*., **15**, 108 (1994).
51. Nagender Naidu S.V. and Rama Rao P., *Phase Diagrams of Binary Tungsten Alloys*, Indian Institute of Metals, Calcuta, 1991, p. 122.
52. Moser Z. and Gumiński C., *J. Phase Equil.*, **14**, 726 (1993).
53. Gumiński C., *ibid*., **14**, 220 (1993).
54. Gumiński C., *ibid*., **23**, 184 (2002).
55. Gumiński C., *Phase Diagrams of Binary Iron Alloys*, H. Okamoto, Ed., American Society for Materials, Materials Park, 1993, p. 174.
56. Gumiński C., *J. Phase Equil*., **16**, 83 (1995).
57. Gumiński C., *ibid*., **16**, 81 (1995).
58. Gumiński C., *ibid*., **14**, 643 (1993).
59. Gumiński C., *ibid*., **24**, 373 (2003).
60. Gumiński C., *ibid*., **23**, 537 (2002).
61. Milare E., Fertonani F.L., Benedetti A.V. and Ionashiro M., *J. Thermal Anal. Calor*., **59**, 617 (2000).
62. Gumiński C., Lee S.Y. and Nash P., *Phase Diagrams of Binary Nickel Alloys*, American Society for Materials, Materials Park, 1991, p. 167.
63. Gumiński C., *Bull. Alloy Phase Diagr.*, **11**, 22 (1990).
64. Barański A., Kryska A. and Galus Z., *J. Electroanal. Chem.*, **349**, 341 (1993).
65. Gumiński C., *J. Less-Common Met*., **168**, 329 (1991).
66. Gumiński C., *Bull. Alloy Phase Diagr.*, **11**, 26 (1990).
67. Chakrabarti D.J., Gumiński C. and Laughlin D.E., *Phase Diagrams of Binary Copper Alloys*, American Society for Materials, Materials Park, 1994, p. 205.
68. Baren M.R., *J. Phase Equil*., **17**, 122 (1996).
69. Okamoto H. and Massalski T.B., *Bull. Alloy Phase Diagr.*, **10**, 50 (1989).
70. Zabdyr L.A. and Gumiński C., *J. Phase Equil*., **16**, 353 (1995).
71. Gumiński C. and Zabdyr L.A., *ibid*., **13**, 401 (1992).
72. Gumiński C., unpublished.
73. McAlister A.J., *Bull. Alloy Phase Diagr.*, **6**, 219 (1985).
74. Gumiński C. and Zabdyr L.A., *J. Phase Equil*., **14**, 719 (1993).
75. Okamoto H., *Phase Diagrams of Indium Alloys*, American Society for Materials, Materials Park, 1991, p. 129.
76. Gumiński C., *J. Phase Equil*., **15**, 111 (1994).
77. Gumiński C., *ibid*., **14**, 219 (1993).
78. Gumiński C., *ibid*., **22**, 682 (2001).
79. Gumiński C., *ibid*., **20**, 344 (1999).
80. Zabdyr L.A. and Gumiński C., *ibid*., **14**, 743 (1993).
81. Zabdyr L.A. and Gumiński C., *ibid*., **14**, 734 (1993).

82. Gumiński C., *ibid*., **18**, 101 (1997).
83. Gumiński C., to be published.
84. Gumiński C., *J. Phase Equil*., **17**, 419 (1996).
85. Gumiński C., *Bull. Alloy Phase Diagr.*, **11**, 317 (1990).
86. Zabdyr L.A. and Gumiński C., *J. Phase Equil*., **17**, 230 (1996).
87. Gumiński C., *ibid*., **20**, 85 (1999).
88. Sharma R.C., Chang Y.A. and Gumiński C., *ibid*., **14**, 100 (1993).
89. Sharma R.C., Chang Y.A. and Gumiński C., *ibid*., **13**, 663 (1992).
90. Sharma R.C., Chang Y.A. and Gumiński C., *ibid*., **16**, 338 (1995).
91. Gumiński C., *ibid*., **16**, 337 (1995).
92. Gumiński C., *ibid*., **22**, 578 (2001).
93. Gumiński C., *ibid*., **15**, 101 (1994).
94. Gumiński C., *ibid*., **21**, 539 (2000).
95. Gumiński C., *ibid*., **18**, 206 (1997).
96. Gumiński C., *ibid*., **16**, 525 (1995).
97. Gumiński C., unpublished.
98. Gumiński C., *J. Phase Equil*., **17**, 442 (1996).
99. Gumiński C. and Galus Z., *Intermetallic Compounds in Mercury*, *IUPAC Solubility Data Series*, Vol. 51, J.G. Osteryoung and M.M. Schreiner, Eds., Pergamon, Oxford, 1992.
100. Gumiński C., *Z. Metallk*., **77**, 87 (1986).
101. Galus Z., *Pure Appl. Chem*., **56**, 635 (1984).
102. Gumiński C. and Galus Z., *J. Electroanal. Chem*., **83**, 139 (1977).
103. Igolinskii V.A. and Shalaevskaya V.N., *Elektrokhimiya*, **10**, 536 (1974).
104. Gumiński C., *J. Mater. Sci*., **24**, 2661 (1989).
105. Lou L., Xu Y.-X and Zhang C.-G., *Fenxi Huaxue*, **27**, 162 (1999).
106. Makarova I.A., Lange A.A. and Bukhman S.P., *Izv. Akad. Nauk Kaz. SSR, Ser. Khim*., no 6, 35 (1990).
107. Xu Y.-X., and Zhang C.-G., *Gaodeng Xuexiao Huaxue Xuebao*, **17**, 1711 (1996).
108. Zhang C.-G., Xu Y.-X. and Mu L., *ibid.*, **14**, 1111 (1993).
109. Lu W. and Baranski A.S., *J. Electroanal. Chem*., **335**, 105 (1992).
110. Korshunov V.N., Khlystova K.B., Kraev V.A. and Vacherikova S.G., *Elektrokhimiya*, **21**, 1233 (1985).
111. Tamamushi R., *J. Electroanal. Chem*., **109**, 353 (1980).
112. Chlistunoff J., *Doctor thesis*, University of Warsaw, Poland, 1988.